Full Papers
doi.org/10.1002/ejic.202100510

Determination of Stereoelectronic Properties of NHC Ligands *via* Ion Pairing and Fluorescence Spectroscopy

Stepan Popov[a] and Herbert Plenio*[a]

We present an experimental method, which provides information on the steric and electronic properties of ligands in metal complexes. This approach is based on the equilibrium of ion-pairing of a cationic $[(NHC)Ir(cod)]^+$ and a fluorescent bodipy-sulfonate ($bdpSO_3^-$). The close ion-pair of [(NHC)Ir($bdpSO_3$)(cod)] in toluene solution is weakly fluorescent, but dissociates into solvent-separated ion pairs upon exposure to slightly more polar solvents. This spatial separation leads to a very pronounced increase of the fluorescence. The separation into distinct ions depends on the polarity of the solvent, but more importantly also on the stereoelectronic properties of the NHC ligand. 26 different NHC ligands with varying steric and electronic properties were probed in 1,2-dichloroethane solvent. The electronic properties of the ligands were examined *via* the established descriptors (redox potential and ν(CO)). The systematic variation of NHC donation enables the deconvolution of electronic and steric contributions of the respective ligand.

Introduction

Numerous experimental and theoretical methods are used for the determination of the electronic and steric properties of N-heterocyclic carbenes ligands to transition metals.[1] The classic Tolman approach based on $[(NHC)Ni(CO)_3]$ complexes utilizing ν(CO) is still valuable and provides information on the net electron density transferred from the NHC ligand to the metal center. This approach is less convenient with a view to the extreme toxicity of $Ni(CO)_4$[2] and has largely been replaced by a closely related method based on work by Crabtree et al. utilizing other carbonyl complexes $[(NHC)M(CO)_2X]$ (M = Rh, Ir and X = Br, Cl).[3] This approach was later unified by Nolan et al. enabling the correlation of the Ni- and the Rh-carbonyl scale,[4] while Plenio and Wolf linked the Rh- and Ir-based scales to the Tolman parameters.[5] However, the choice of the metal carbonyl was believed to be arbitrary, but Belpassi et al. showed recently, that for $[(NHC)Au(CO)]^+$ complexes the ν(CO) primarily depends on the metal-to-ligand π back-donation.[6]

The redox potentials of [(NHC)IrCl(cod)] complexes are another useful parameter for the determination of electronic properties of NHC ligands.[7] Even though the Ir(I/II) redox potential primarily probes the ability of the ligand to stabilize higher oxidation states at the metal center, this parameter was shown to reflect the respective ν(CO) data.[1a,5] NMR spectroscopy has also been employed to better understand the electronic properties of NHC ligands. The use of ^{13}C chemical shift of the carbene carbon atom in palladium(II)-benzimidazolylidene complexes were suggested by Huynh et al.,[8] while Ganter et al. showed the respective azolium ^{13}C-^{1}H coupling constants to be a measure of the donor capacity of the respective NHC ligands.[9] ^{13}C-NMR was proposed by Tarantelli, Belpassi et al. to measure σ-donor properties of NHC ligands in gold(I) complexes.[10]

The NMR shifts of the ^{31}P NMR resonances in phosphinidene complexes and of the ^{77}Se resonances in selenoureas were proposed by Bertrand et al.[11] and Ganter et al.[12] as a measure of the π-accepting abilities of the respective NHC ligands. DFT calculations by Cavallo et al. support the usefulness of this method,[13] while Huynh points to some inconsistencies, possibly due to the interference of steric effect on the ^{77}Se NMR shifts.[1b] Bond dissociation energies of carbonyl gold complexes have also been proposed as a measure for ligand effects including NHC ligands.[14]

Methods for the determination of the steric properties of NHC ligands are much less common.[15] The simple Tolman approach based on CPK-models is not applicable to NHC ligands, due to the primarily C_2-symmetric shape of such ligand. Cavallo et al. developed the buried-volume approach, which provides a good description of the steric properties of NHC ligands and relies on solid state coordinates obtained from X-ray crystal structure analysis, for which single crystals of the respective complex are needed.[16] In this concept the metal is located at the center of a sphere (default radius 350 pm) and is coordinated by an NHC ligand (metal-C(NHC) = 200 or 228 pm reflecting the size of different metals).[17] The buried volume (% V_{bur}) is the fraction of the volume of the sphere, which is occupied by the atoms of the NHC ligands (excluding the hydrogen atoms).[18] A detailed analysis of the scope and the limitations of the buried-volume method was provided by Gomez-Suarez, Nelson and Nolan.[1e] A significant problem of this approach is the treatment of conformationally flexible

[a] S. Popov, Prof. Dr. H. Plenio
Organometallic Chemistry,
Technical University of Darmstadt,
Alarich-Weiss-Str. 12, 64287 Darmstadt, Germany
E-mail: plenio@tu-darmstadt.de

Supporting information for this article is available on the WWW under https://doi.org/10.1002/ejic.202100510

molecules, since the buried volume provides data only for the conformation observed in the solid state and does not take into account the conformational degrees of freedom of a molecule in solution.

In a refined approach Cavallo et al. later introduced topographic steric maps which contain altimetric isocontour lines offering a quantitative description of the catalytic pocket[19] to account for variable steric effects in different areas around the metal center. This approach is applicable to a wide range of different metal-ligand complexes and is aiming at the computer-aided design of catalytic pockets.[20] Despite the huge success of this approach, the analysis of the steric environment of the metal center still relies on the static coordinates typically obtained from X-ray crystal structure analysis or DFT. Molecular dynamics, leading to changes in the shape and the accessibility of the pocket are not taken into account. In an attempt to consider conformative flexibility for metal-ligand design Patton et al. recently reported on Boltzmann-weighted Sterimol parameters useful in multivariate models of enantioselectivity.[21] Alternatively, Gusev developed a parameter *r* as a measure of the direct repulsive interactions between a NHC ligand and CO ligands in [(NHC)Ni(CO)$_3$]. Such parameters are also needed to analyze and predict ligand and catalyst effects in organometallic catalysis.[22]

In order to account for the structural dynamics of metal complexes in solution, we wish to present here an experimental method, which provides information on the steric and electronic properties of ligands in metal complexes. This approach is based on the equilibrium of ion-pairing of a cationic [(NHC)Ir(cod)]$^+$ and a fluorescent bodipy-sulfonate (bdpSO$_3^-$). Electron-rich iridium in [(NHC)IrX(cod)] complexes is known to PET-quench (photoinduced electron transfer) the fluorescence of a fluorophore bonded to this complex.[23] This quenching is distance-dependent and it is dominant at iridium-fluorophore distances smaller than 1 nm.[24] In previously synthesized complexes the nature of the covalent linker connecting NHC ligand and fluorophore determines the average distance between the fluorophore and the iridium quencher and it also determines the brightness of the fluorophore. Now we report on complexes in which the distance between fluorophore (anion) and quencher (cation) is variable and in which the degree of ion-pairing depends not only on the solvating nature of the solvent, but also on the stereoelectronic properties of anion and cation. For complexes of the general type LM$^+$ X$^-$ dissolved in a defined solvent and with variable L this approach provides a convenient handle to probe the stereoelectronic properties of ligand L.

Results and Discussion

Several of the known methods for the determination of the electronic properties of NHC ligands utilize [(NHC)IrCl(cod)] and the closely related [(NHC)IrCl(CO)$_2$] complexes.[1e] It is convenient, that the fluorescence method described here also relies on [(NHC)IrCl(cod)] complexes for which the chloride ligand is simply replaced by the weakly coordinating bdpSO$_3^-$- (Scheme 1). The sulfonated bodipy was synthesized according to a general procedure by Burgess.[25] Quenching of the in-situ formed sulfonic acid with Ag_2CO_3 provides the respective silver sulfonate. In order to cover a wide range of electronic and steric properties of NHC ligands, the silver sulfonate was reacted with a large number of [(NHC)IrCl(cod)] complexes (Scheme 2) to render the respective [(NHC)Ir(bdpSO$_3$)(cod)] (X = Cl$^-$, bdpSO$_3^-$) according to established general procedures.[7a,26] The sulfonate complexes were synthesized in virtually quantitative yield according to Dorta et al., who had studied in detail the reactions of [(NHC)IrCl(cod)] complexes with different silver salts containing weakly coordinating anions in CH_2Cl_2/CH_3CN solution.[27]

In non-polar solvents the sulfonate complex forms close ion-pairs[28] and due to the short distance between fluorophore and iridium the fluorophore is quenched – presumably via a PET mechanism.[24] The fluorescence is restored in slightly more polar solvents, since solvent separated ions are formed for which the distance between quencher and fluorophore is too large to significantly influence the fluorescence properties. Consequently, monitoring the fluorescence of such complexes under various conditions is going to provide information on the degree of ion-pairing in such complexes. This ion-pairing depends on the nature of the solvent and (more importantly) on the stereoelectronic properties of the NHC ligand in [(NHC)Ir(bdpSO$_3$)(cod)] complexes. Based on this concept, we have systematically probed the stereoelectronic properties of 26 NHC ligands by measuring their fluorescence under various conditions (Scheme 2).

Solvent-titration experiments. Initially, toluene solutions of different [(NHC)Ir(bdpSO$_3$)(cod)] complexes ($c = 1.0 \cdot 10^{-6}$ mol/L)

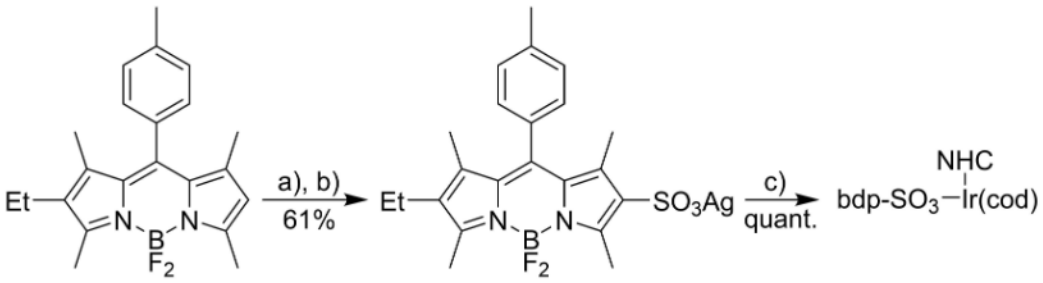

Scheme 1. Synthesis of bdpSO$_3$Ag a) ClSO$_3$H, CH_3CN, $T = -40$ °C, b) Ag_2CO_3, rt, c) [(NHC)IrCl(cod)] (cod = 1,5-cyclooctadiene), MeCN/CH_2Cl_2.

Full Papers
doi.org/10.1002/ejic.202100510

Chemistry Europe
European Chemical Societies Publishing

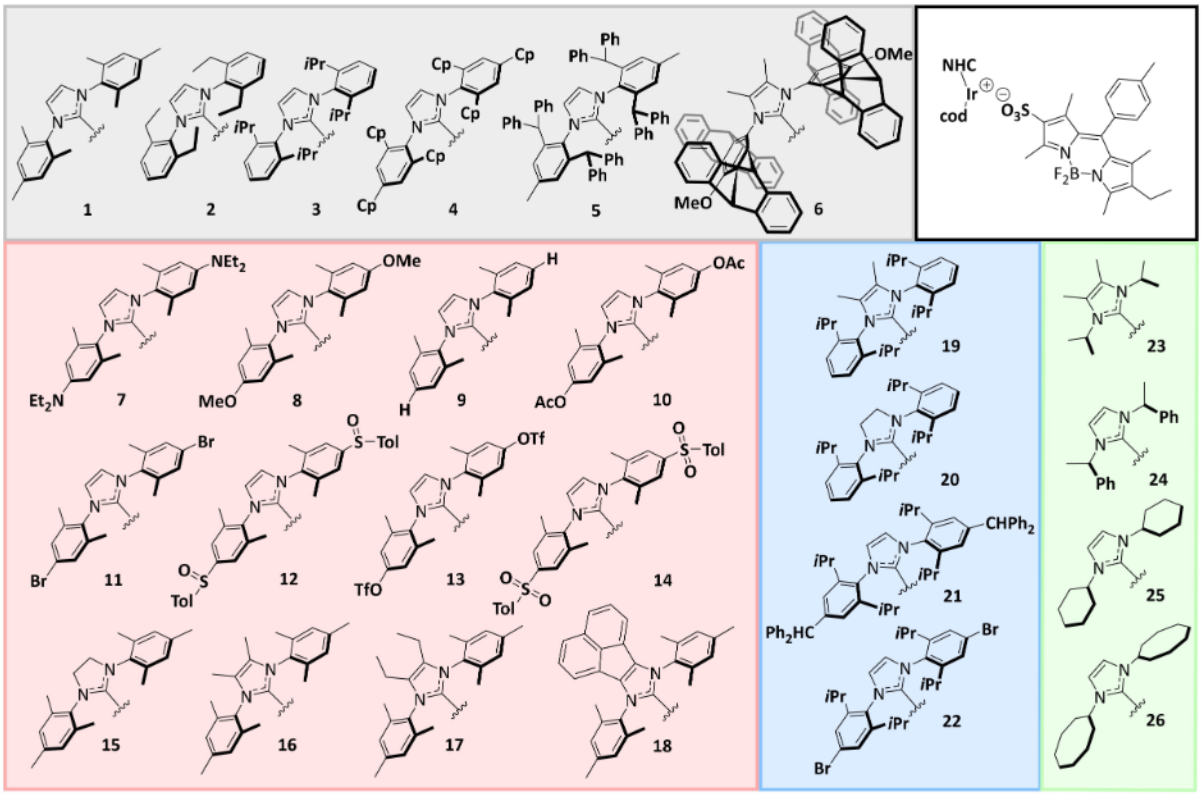

Scheme 2. List of (NHC)Ir complexes employed for the analysis of stereoelectronic properties.

were titrated with DMAc and the fluorescence determined after each addition (Figure 1). The initial fluorescence (without any added DMAc) is weak, since anion and cation form close ion-pairs in which iridium quenches the fluorophore. Nonetheless,

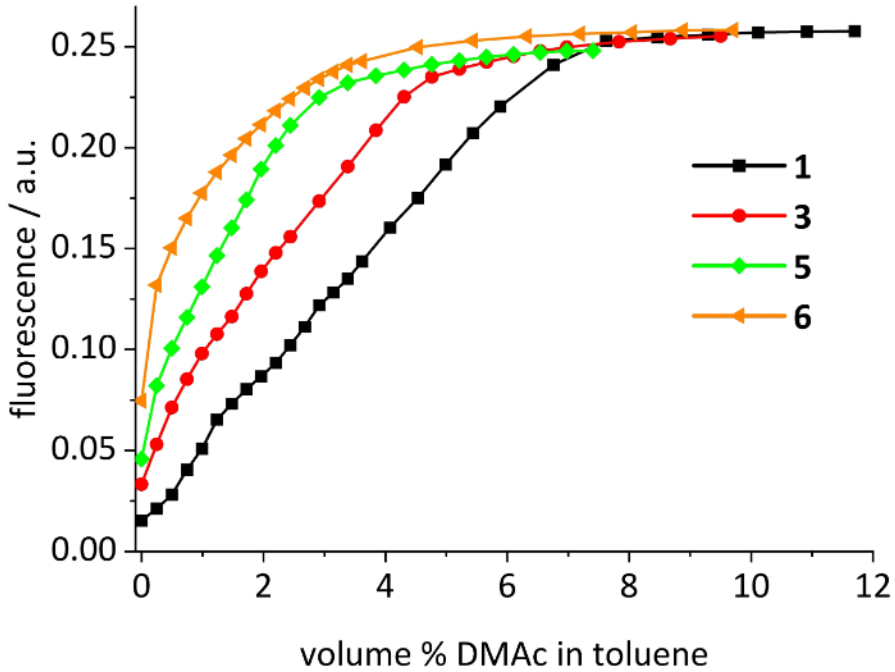

Figure 1. Fluorescence of complexes [(NHC)Ir(bodipySO_3)(cod)] (NHC = **1**, **3**, **5** and **6**) (complex initial $c = 1.0 \cdot 10^{-6}$ mol/L) in toluene with addition of DMAc (fluorescence dilution corrected).

even the toluene solutions show slightly different fluorescence levels, which appear to be sorted according to the steric bulk of the respective NHC ligand. The Ir complexes **5** and **6** with two bulkiest NHC ligands display the most intense toluene fluorescence. It seems that even in non-polar toluene a the complexes are characterized by a different degree of anion-cation contacts.[29] The addition of polar solvent (DMAc) to a toluene solution leads to an up to 12-fold increase in the fluorescence (Figure 1). The final intensity corresponds to the fluorescence of the fully separated ion-pair, which is the same regardless of the nature of the initial complexes. The effect of steric bulk on the ion pairing is again visible, since complexes with bulky NHC ligands reach the maximum fluorescence much earlier - i.e. upon addition of less polar DMAc than complexes with less bulky NHC ligands. These preliminary experiments illustrate the sensitivity of the fluorescence signal with respect to the nature of the NHC ligand.

Probing the Ir(I/II) redox potentials. In order to distinguish between steric and electronic effects of the NHC ligands on ion-pairing, the electronic properties of all NHC ligands employed in this study need to be determined. The M(I/II) redox potentials of [(NHC)MCl(cod)] (M = Ir, Rh) were previously established to be a measure of the electron donating ability of the respective NHC ligands.[5,7a] The respective Ir(I/II) redox potentials of all [(NHC)IrCl(cod)] complexes (Scheme 2) were measured or taken from the literature (Table 1).

With the exception of three N-alkyl NHC complexes (**24**, **25**, **26**), the electrochemistry of the iridium complexes is well behaved. The complexes are characterized by reversible redox waves with oxidation/reduction wave separations in the range of 64–96 mV. In the full data set, several subsets can be identified (eg IMes series and IPr series), in which substituents at certain positions are changed in a systematic manner, to change NHC donation while the steric bulk of the NHC ligand remains constant. The influence of the various *p*-R substituents in the N-aryl NHC complexes on the Ir(I/II) redox properties is pronounced. This is evidenced by the almost 300 mV range of the redox potentials depending on the nature of the substituents – despite the fact, that the N-aryl rings are orthogonal to the respective central imidazolylidene ring. There is considerable evidence in the literature, that the N-aryl rings are able to directly interact with the metal center via π-face interactions[7b,31] leading to an efficient transfer of electronic information between the N-aryl ring and the metal center.

Complexes **7**–**14** are structurally very similar and only differ with respect to the nature of the *p*-substituent at the N-aryl rings (*p*-R = NEt_2, OMe, H, Br, OAc, SOtol, OTf, SO_2tol) of the imidazolylidene. For complexes **7**–**14**, an excellent correlation of Hammett parameters of the nature of the *p*-R substituents and redox potentials was observed (Figure 2). The closely related IPr-series of complexes (**3**, **19**, **21**, **22**) display analogous changes in the redox potentials. A note concerning the Hammett constant of –OC(O)Me is required. The tabulated value for this group is $\sigma_p = 0.31$,[32] which would make it an outlier in Figure 2. But this value may not be correct since it is unlikely, that the acetoxy group is more electron withdrawing than the closely related –OC(O)Ph substituent ($\sigma_p = 0.13$). This peculiarity concerning the acetoxy substituent was noted previously by Papp et al. and a revision of the respective Hammett constant suggested;[33] their value ($\sigma_p = -0.08$) is used in Figure 2.

Table 1. Redox potentials of [(NHC)IrCl(cod)] complexes in 1,2-dichloroethane (rt, supporting electrolyte $NnBu_4PF_6$ 0.1 M) and referenced against the formal potential of octa-methylferrocene ($FcMe_8$ $E_{1/2} = -0.01$ V) (previously reported redox potentials are denoted as: L = Ref. [7a]; S = Ref. [30]) and rel. fluorescence intensities $I_{rel} = I/I_{end}$. The $\nu(CO)_{av}$ from [(NHC)IrCl$(CO)_2$] complexes and fluorescence from [(NHC)Ir(bdpSO_3)(cod)]. Literature sources for the buried volumes (experimental and DFT): supporting information. For the buried volume data Au = [(NHC)AuX], Ir = [(NHC)IrCl(cod)] and Ag = [(NHC)AgCl].[a]

	$\triangle E_{1/2}$ [V]	E_a-E_c [mV]	$\nu(CO)_{av}$ [cm^{-1}]	I_{rel} [%]	V_{bur} [%]
1 (IMes)	0.765^{L}	80	2023.3	16.2	36.5^{Au} 33.0^{Ir}
2 (IEt)	0.748	76	2023.4	17.9	31.7^{Ir}
3 (IPr)	0.762	82	2023.8	70.7	45.4^{Au}
4 (2,4,6-Cp)	0.737	66	2021.3	64.6	
5 (2,6-$CHPh_2$)	0.863	75	2026.0	88.0	50.4^{Au}
6 (N,N-Pentiptycenyl)	0.804^{S}	81	2024.3	84.1	48.8^{Ag}
7 (*p*-NEt_2)	0.648^{L}	80	2021.0	58.1	31.6^{Ir}
8 (*p*-OMe)	0.757	96	2022.8	26.7	
9 (*p*-H)	0.786^{L}	78	2024.0	16.5	31.6^{Ir}
10 (*p*-OAc)	0.793	92	2025.1	14.8	31.7^{Ir}
11 (*p*-Br)	0.862^{L}	78	2025.5	10.8	31.7^{Ir}
12 (*p*-SOTol)	0.870^{L}	72	2028.5	11.4	
13 (*p*-OTf)	0.903	88	2027.4	8.8	31.8^{Ir}
14 (*p*-SO_2Tol)	0.920^{L}	80	2029.5	8.3	
15 (SIMes)	0.735	76	2024.5	22.3	36.9^{Au}
16 (Me bb)	0.692	83	2020.3	30.5	31.4^{Ir}
17 (Et bb)	0.681	95	2021.1	33.2	31.6^{Ir}
18 (1,8-naphtadiyl bb)	0.770	73	2022.8	17.3	
19 (IPr (Me bb))	0.720	96	2021.3	81.1	
20 (SIPr)	0.744	81	2024.9	71.7	47.0^{Au}
21 (IPr (*p*-$CHPh_2$))	0.777	64	2023.3	66.5	
22 (IPr (*p*-Br))	0.870	96	2025.8	57.9	
23 (N-*i*PrMe)	0.754	75	2020.8	15.9	38.5^{Au}
24 (N-EtPh)	0.82[a)]	93	2026.3	14.6	36.4^{Au}
25 (N-Cyclohexyl)	0.79[a)]	123	2022.3	14.2	27.5^{Au}
26 (N-Cyclooctyl)	0.83[a)]	117	2021.3	12.0	

[a] CV not fully reversible.

The redox potentials are sensitive to small changes of the N-aryl substituents: Complexes **1** ($E_{1/2} = 0.765$ V), **2** ($E_{1/2} = 0.748$ V) and **3** ($E_{1/2} = 0.762$ V) serve as an instructive example: Complex **1** has three methyl groups on each N-aryl ring, complex **2** has two ethyl groups and complex **3** has two isopropyl groups on each N-aryl ring.

The donation of NHC ligands can also be modulated via substituents in the backbone of the imidazolylidene unit.[34] Complexes **1**, **16**, **17** and **18** constitute another mini-series and differ only concerning the backbone substituents (R_{bb} = H, Me, Et and 1,8-naphthadiyl). Backbone substituents have a stronger influence on the redox potentials than 4-R substituents (the effect of two 4-R methyl groups is 21 mV, while two backbone methyl groups lead to a cathodic shift of the redox potential of 73 mV). Based on this, the backbone modulated NHC ligands fill the large gap in electronic properties of the NHC ligands between *p*-NEt_2 (Table 1, complex **7**) and *p*-OMe (Table 1, complex **8**). Variation of the backbone substituents in N-aryl

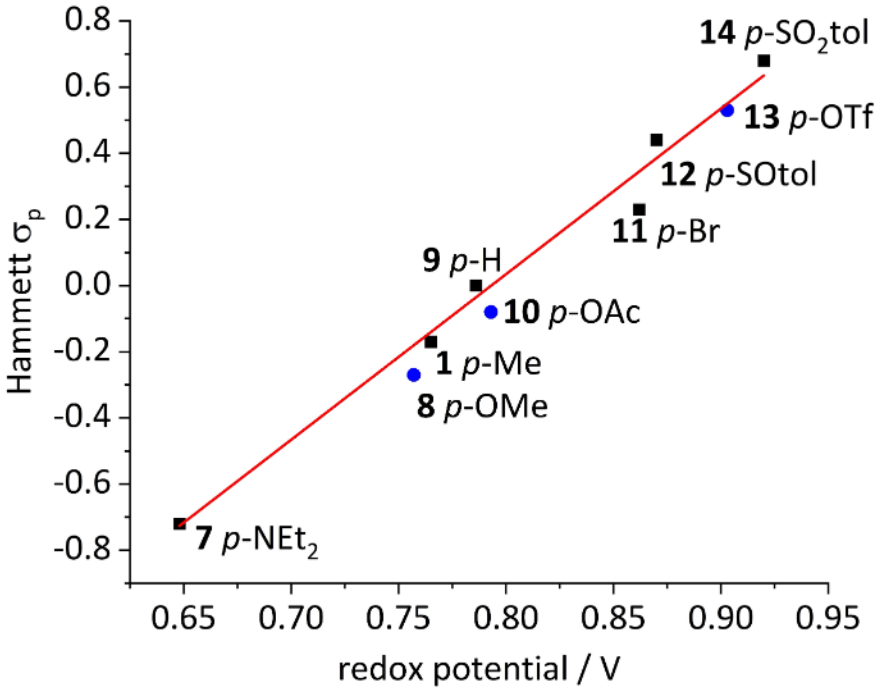

Figure 2. Plot of the Hammett constants of the respective *p*-R substituents and the redox potentials for [(NHC)IrCl(cod)] (NHC = **7–14**) (previously reported redox potentials black squares, newly determined redox potentials blue circles).

NHC ligands were previously shown to have no significant effect on the steric bulk.[1e,35] Consequently, the steric bulk of the NHC ligands in complexes **7–14**, **16** and **17** is very similar and the NHC ligands primarily differ with respect to the electronic properties. The remaining complexes in Table 1 show less variation in the electronic properties and more steric variations. Most redox potentials are within expectations based on the nature of the NHC-substituents. For a few complexes significant deviations from the expected redox potentials were observed (complex **5** and **6**), which will be discussed later in the context of infrared spectroscopy-based determinations of NHC electronic parameters.

The cyclic voltammograms of the N-alkyl NHC complexes **24**, **25** and **26** are not fully reversible, thus the Ir(I/II) redox potentials lack precision. The redox potential of those N-alkyl NHC complexes show nearly the same redox potentials. Complex **23** is oxidized at considerably more cathodic redox potential ($E_{1/2}$ = 0.754 V) - again the effect of the two backbone methyl groups on the redox potential is significant.

Fluorescence measurements. The fluorescence of the various complexes **1–26** ($c = 1.0 \cdot 10^{-6}$ mol/L) were determined in four different solvent (mixtures): toluene, toluene – dce (1:1 vol.), toluene-dce (1:2 vol.) and in dce (1,2-dichloroethane) solution. For all complexes the fluorescence intensities increase in this order. To minimize small weighing and pipetting errors as well as changes in the intensity of the excitation light source, the fluorescence intensities are always given relative to the values for the fully separated ion pairs. This is easily achieved by adding a very small amount of NBu_4Br -solution at the end of each experiment. The strongly coordinating bromide quantitatively displaces the $bdpSO_3^-$ from the iridium coordination sphere, which is resulting in the spatial separation of quencher and fluorophore.

The fluorescence of the solutions of the different complexes ($c = 1.0 \cdot 10^{-6}$ mol/L) is in the ideal range of ca. 10%–90% of the maximum fluorescence. Consequently, the apparent equilibrium constant according to the simplest equilibrium reaction $MX = M^+(solv) + X^-(solv)$ describing the dissociation of the close ion-pair, has to be in the range of the inverted concentration of the initial complex. Based on this, the highly sensitive fluorescent based method is ideal for investigating ion dissociation of the [(NHC)Ir($bdpSO_3$)(cod)] with variable NHC ligands. However, care needs to be exercised concerning the aforementioned equilibrium constants. As pointed out by Gibson et al.[36] such ionic equilibria in non-polar solvents are not as simple as for polar solvents. Due to the poorly solvating nature of the non-polar solvents, aggregates such as M_2X^+ or MX_2^- with modulated fluorescence or different types of solvent-shared ion pairs complicate the simplistic approach.[28,37] More importantly, the activity coefficients of ions in non-polar solvents with low dielectric constants are exponentially related to the inverse 3/2 power of the permittivity and because of this, the activity coefficient is extremely sensitive to ionic strength in such solvents.[38] In line with this we have observed a concentration dependence of the apparent equilibrium constants in our experiments, when studying ion separation at different concentration to determine equilibrium constants. A rigorous analysis of the multiple equilibria is beyond the scope of this study – and it is also not needed for evaluating the stereoelectronic properties of the NHC ligands, since the fluorescence provides

sufficient information for comparison among the different metal complexes once this is done at a constant concentration of the salt.[39]

Most complexes of the IMes series display only weak fluorescence in solvents other than pure dce (Figure 3). The dissociation of the complexes into separated ions pairs is not pronounced due to the moderate steric bulk of the NHC ligands – with the exception of the most electron-rich complex **9**. Since the steric bulk of the different NHC ligands in the IMes series is very similar, the fluorescence modulation is predominantly caused by the different donation of the IMes-type NHC ligands. Obviously, in the more electron-rich complexes the dissociation into solvent-separated ions is facilitated, since electron-rich NHC substituents stabilize the respective cationic iridium complex.

Correlation of redox potentials and fluorescence data. In order to resolve the combined influence of sterics and electronics on the fluorescence of the respective [(NHC)IrX(cod)] complexes, the Ir (I/II) redox potential (as a descriptor of the electronic properties of NHC ligands) and the fluorescence are correlated. The plot of redox potentials $\Delta E_{1/2}$ and the relative fluorescence intensities (I_{rel}) for complexes of the electronic subset (Figure 4, red data set for IMes-type complexes and blue data set for IPr-type complexes) can both be fitted with simple exponential functions.[40] Alternatively, based on $\ln(K) \approx \Delta E$, a linear plot is shown in Figure 5.[41]

The only outlier in the red series of complexes is complex **7**. We consider it less likely, that the higher-than-expected fluorescence is caused by the interaction of the cationic Ir with the weakly coordinating aryl-NMe_2 substituent. In the various solvent titration experiments with acetamides the addition of such small amounts of donating ligand has no measurable influence on the fluorescence (Figure 1). Eventually, the basic nitrogen atom is partially protonated by adventitious acid (CO_2/H_2O) and the derived counter anion interferes with the $bdpSO_3$ coordination. Such contamination cannot be excluded with certainty, since the experiments are done in very dilute (micromolar) solutions.

Based on the analysis of red set of metal complexes containing ligands with variable donicity but similar sterics, it is possible to deconvolute the steric and the electronic influence of NHC ligands in the respective metal complexes. The vertical distance (Δ log I_{rel}%) between the red linear fit curve (Figure 5) may be used as a relative steric denominator termed Fluobulk (fluorescence bulk) given relative to the IMes series of complexes. For example, for complexes **3** (Fluobulk = +1.28), **4** (Fluobulk = +1.03), **5** (Fluobulk = +1.17) and **6** (Fluobulk = +1.34). Based on this the pentiptycene based NHC ligand is by far the bulkiest NHC ligand studied here.

The data set in Figure 5 contains more interesting subsets. The series of complexes **1** and **2** are IMes type complexes, which are characterized by the different ortho- substituents R = Me and Et. The fluorescence of **1** and **2** are virtually identical (after correction according to linear fit curve),[42] meaning that the steric effect of the ethyl group relative to the methyl group is negligible. This may explain, why the ortho-ethyl substituted NHC ligands are rarely used in catalysis. It is difficult to compare to literature data, since crystal structure and DFT-derived differ significantly.[26b] In the solid state this buried volume will depend very much on the orientation of the terminal $-CH_3$ group relative to the metal center. For the ion pairing the orientation of this $-CH_3$ groups close to the metal center appears to play only a very minor role.

The four complexes with N-alkyl substituents (**23**, **24**, **25**, **26**) are characterized by modest levels of fluorescence ranging from 12.0–15.9%. This series of complexes is interesting, since significant discrepancies of the buried volume approach and the ion-pair dissociation approach become apparent. Based on

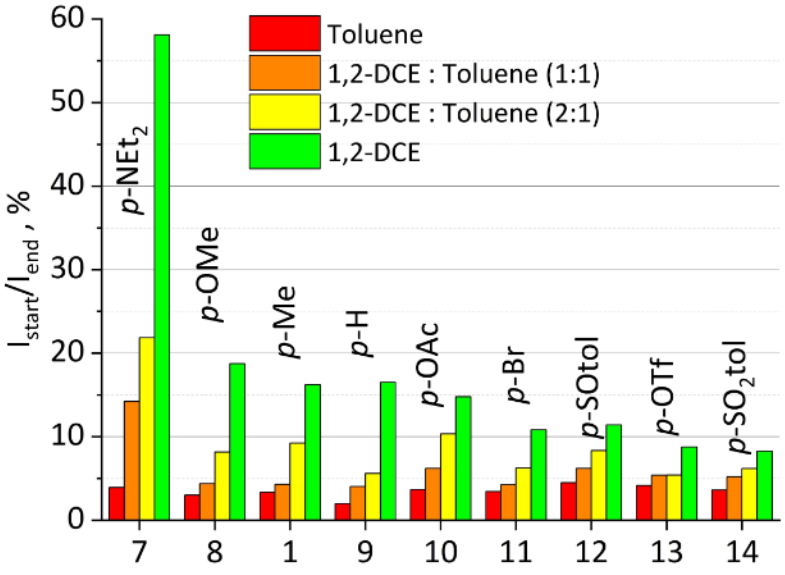

Figure 3. Plot of the relative fluorescence ($I_{rel} = I/I_{max}$) for the complexes [(NHC)Ir($bdpSO_3$)(cod)] (NHC = **1**, **7–14**) of the IMes series in four different solvents. In **red** color are initial intensities in toluene, in 1,2-dichloroethane-toluene (1:1)(orange), in 1,2-dichloroethane-toluene (2:1)(yellow), in 1,2-dichloroethane (green).

Full Papers
doi.org/10.1002/ejic.202100510

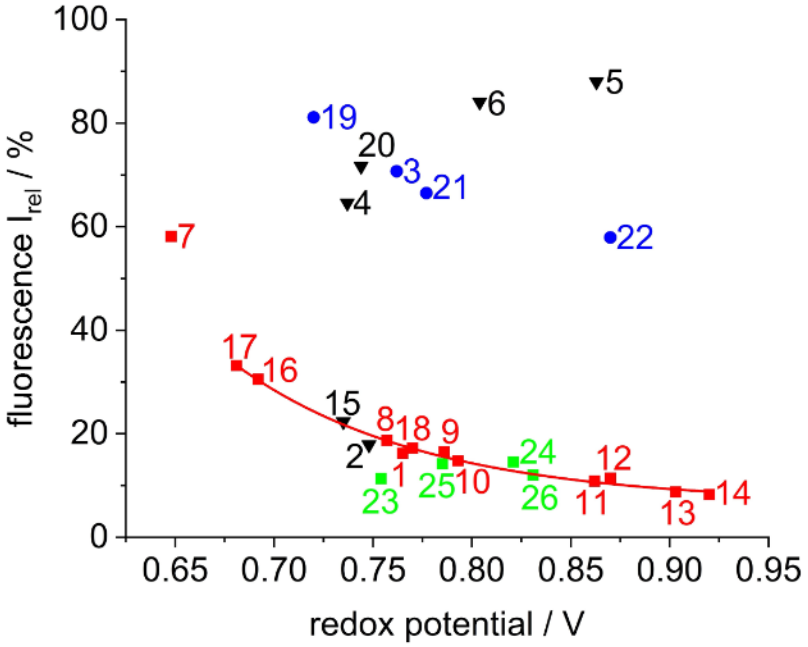

Figure 4. Plot of relative fluorescence intensity (I_{rel}) of [(NHC)Ir(bdpSO$_3$)(cod)] in 1,2-dichloroethane vs. the redox potentials for [(NHC)IrCl(cod)] in CH_2Cl_2. The data of the IMes electronic series, backbone substituted complexes and the respective exponential fit ($R^2 = 0.99$) are drawn in red color; IPr complexes (NHC = **3**, **19**, **21**, **22**) (blue circles); N-alkyl NHC data (green squares), remaining complexes (black triangles).

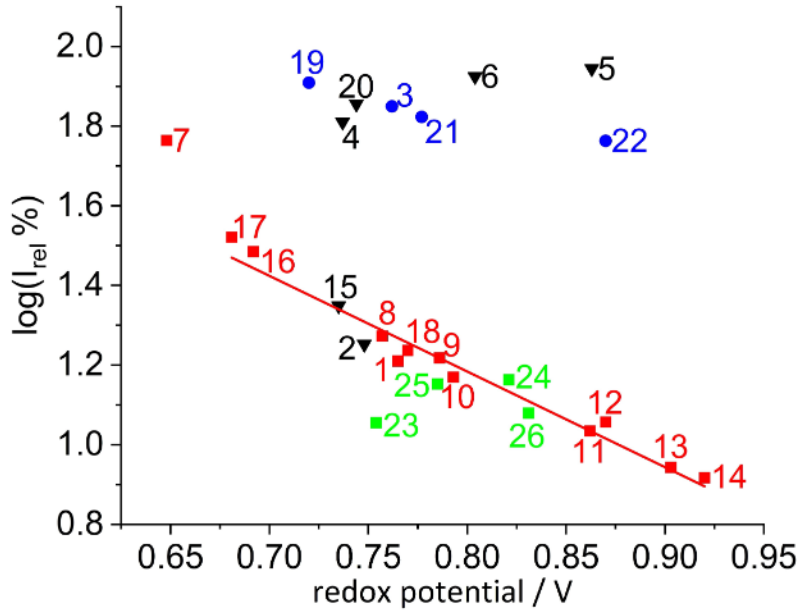

Figure 5. Plot of log relative fluorescence intensity (log I_{rel}) of [(NHC)Ir(bdpSO$_3$)(cod)] vs. redox potentials for [(NHC)IrCl(cod)] in 1,2-dichloroethane. Color coding see legend to Figure 4. Linear regression: $y = 3.106–2.402 \cdot x$ ($y = \log(I_{rel}\%)$; $x =$ redox potential).

the fluorescence (Figure 5) and based on the buried volumes (Table 1), the NHC ligands in complex **24** and **1** display similar size. The buried volume provided in Table 1 (entry 24) was determined for the imidazolin-2-ylidne ligands, but it is known, that imidazol-2-ylidene and imidazolin-2-ylidne display very similar buried volumes, which normally differ by less than 1%.[1e] Both NHC in complex **25** (N-Cy^6) and complex **26** (N-Cy^8) are smaller than the NHC in complex **1**, with the N-cyclooctyl NHC being slightly larger than the N-cyclohexyl NHC according to the fluorescence data.

Complex **23** with (N-isopropyl and two backbone methyl groups) is interesting since the observed fluorescence intensity is weak ($I_{rel} = 11.4\%$) and the steric demand of this NHC appears to be much lower than for NHC ligands of the IMes series. This

is in stark contrast to the buried volume of this NHC ligand, which is given as V_{bur} = 38.5 %, while the related complex without backbone methyl groups has V_{bur} = 28.2 %. The reason for the huge buried volume of complex **23** is the solid state structure in which both methyl groups of isopropyl point towards the gold, while H of isopropyl points towards the backbone substituents.[43] The large buried volume of this NHC ligand was discussed by Truscott et al.[44] and according to DFT calculations (B3LYP/6-31 + G*) the isomer with the two methyl groups of the isopropyl group pointing towards the backbone methyl was calculated to be approx. 7 kcal/mol less stable than the 180°-rotamer with the isopropyl hydrogen pointing towards the backbone methyl groups.[45] Based on the fluorescence data reported here it seems, that for the [(NHC)Ir(bdpSO$_3$)(cod)] complexes the rotamer with the methyl groups pointing towards the metal center does not contribute significantly and that the buried volume of NHC **23** is much smaller than previously believed.

Correlation of infrared ν(CO) *and fluorescence data.* The influence of the electronic properties of the NHC ligands on the ion pairing can also be evaluated using the established Tolman electronic parameter or as an equivalent the average of the respective symmetric and antisymmetric ν(CO) in [(NHC)IrCl(CO)$_2$] complexes. This is also helpful, since the electrochemistry of three N-alkyl complexes displays only partial reversibility. In order to obtain a consistent data set minimizing the effect of IR measurements conditions on the ν(CO) no spectroscopic data from the literature were used – except for a few complexes reported by Duckett et al.,[26b] whose IR data for similar complexes are virtually identical to the data measured by us. The data used were taken from our previous reports, missing IR spectra for known or for new complexes were measured under the same conditions to obtain a uniform data set (Figure 6).

Again, the data set is split up in four different subunits: IMes series (red), IPr series (blue), N-alkyl NHC ligands (green) and other complexes (black). The systematic change of NHC donation in the IMes and the IPr series can be fitted with linear functions. As evidenced by the systematic changes in the IMes and IPr series of complexes, this approach appears equally valid – even though the correlation coefficient of the linear fit is significantly smaller than for the redox potential fit. However, it should also be taken into account, that the experimental error of the ν(CO) accounts to at least 1 cm^{-1}.[46] This is significant compared to the signal dispersion, while the error of the redox potential determination relative to the dispersion of the redox potentials is below 10 mV for reversible voltammograms.

The next question concerns the validity of the determined redox potentials. The redox potentials of a few complexes show unexpected values. The redox potential of complex **5** was determined as $E_{1/2}$ = +0.863 V, which is much more anodic than what might be expected based on the four ortho-CHPh$_2$ of the N-aryl ring. Based on the redox potential of complex **21** (containing two para-CHPh$_2$ substituents the -CHPh$_2$ substituent can be considered to be a very weakly electron withdrawing group since the redox potential is shifted by only 29 mV relative to that of complex 20 (has two para-H instead of two para-CHPh$_2$).

The redox potential of complex **6** ($E_{1/2}$ = +0.804 V) is also observed at much higher redox potential than expected – based on the substituents at the N-aryl rings (each N-aryl groups has four donating alkyl substituents and a donating para-OMe group) and the redox potential could have been expected to be at least 100 mv more cathodic. Based on this,

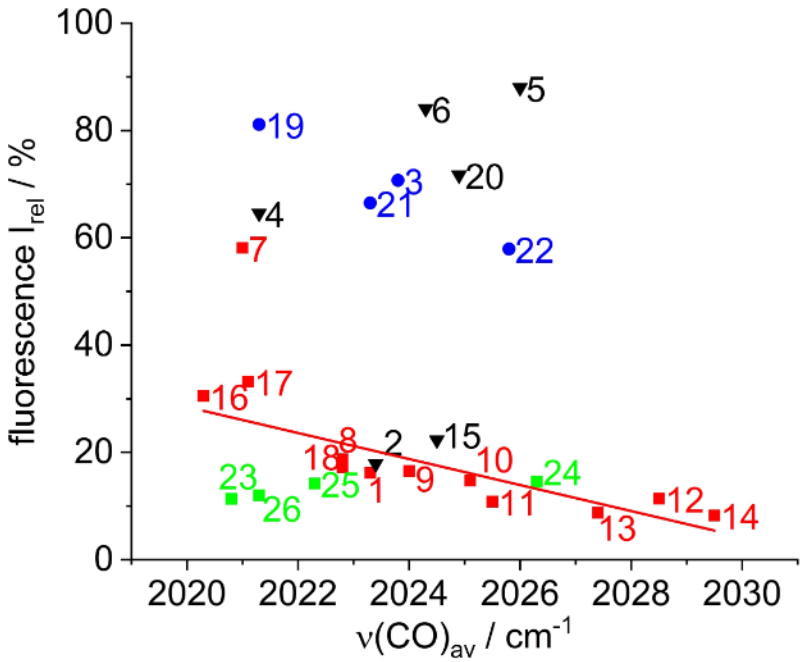

Figure 6. Plot of relative fluorescence intensity (I_{rel}) of [(NHC)Ir(bdpSO$_3$)(cod)] vs. the average of $\nu(CO)_{av}$ for [(NHC)IrCl(CO)$_2$] in CH_2Cl_2. For color coding see legend to Figure 4.

one might argue that the redox potentials of [(NHC)IrCl(cod)] complexes with sterically highly demanding NHC ligands are shifted as a result of the encumbered geometry at the metal center, i.e. that the redox potential depends on the steric bulk of the NHC ligands.

In order to resolve such issues a correlation of the Ir(I/II) redox potentials of [(NHC)IrCl(cod)] complexes and the $\nu(CO)_{av}$ / cm^{-1} of [(NHC)IrCl$(CO)_2$] was done (Figure 7). The linear fit in the plot relies on the red, blue and black data set. For the data points close to the linear fit, the IR spectroscopic data and the redox potentials appear to be correlated and are thus considered valid. Especially the data points for the aforementioned complexes **5** and **6** are very close to the linear fit and the two redox potentials are thus considered to be representative of the "true" NHC donation.

Conclusions

Ion pairing and the derived fluorescence intensity of solutions of [(NHC)Ir(bdpSO$_3$)(cod)] with different NHC ligands depend on the stereoelectronic properties of the NHC ligand. Electron-donating as well as sterically demanding ligands facilitate the formation of solvent-separated ion pairs, which results in the spatial separation of cation and anion. The enlarged distance between fluorophore and the Ir quencher leads to a pronounced increase of the fluorescence signal. Consequently, the stereoelectronic properties of NHC ligands can be determined by measuring the fluorescence intensity of the respective [(NHC)Ir(bdpSO$_3$)(cod)] complexes in dce solution. The linear relationship of redox potential and NHC donation allows the correction of the fluorescence data according to the different donicity of the NHC ligands and reveals the steric bulk of the NHC ligands, which may be quantified by a parameter called Fluobulk. Obvious advantages of the ion pairing approach are, that it is experimentally simple and fast and that the steric information is obtained for complexes in solution. Solid state structures are influenced by packing effects and normally a single conformer is "frozen out". In solution an ensemble of different conformers exists simultaneously, consequently a solution-based approach will provide better data – especially for sterically flexible molecules and for molecules which interact with the solvent.

The approach reported here for the determination of the steric properties of NHC ligands should not be limited to NHC ligands – in principle the steric bulk and the electronic properties of any type of ligand can be studied using a similar approach.

Experimental Section

General experimental. Syntheses were performed in a pre-dried Schlenk flasks under a positive pressure of argon or nitrogen. The flasks were fitted with rubber septa and gas-tight syringes with stainless steel needles or double-cannula were used to transfer air- and moisture- sensitive liquids.

Instrumentations. ^{1}H, ^{19}F and ^{13}C-NMR spectra were recorded on a Bruker DRX 500 or Bruker ARX 300 spectrometer. The chemical shifts are given in parts per million (ppm) on the delta scale (δ) and are referenced to tetramethylsilane (^{1}H, ^{13}C-NMR = 0.0 ppm) or the residual peak of solvent. Abbreviations for NMR data: s = singlet; d = doublet; t = triplet; q = quartet; sep = septet; m = multiplet; bs = broad signal. Mass spectra were recorded on the Bruker Impact II

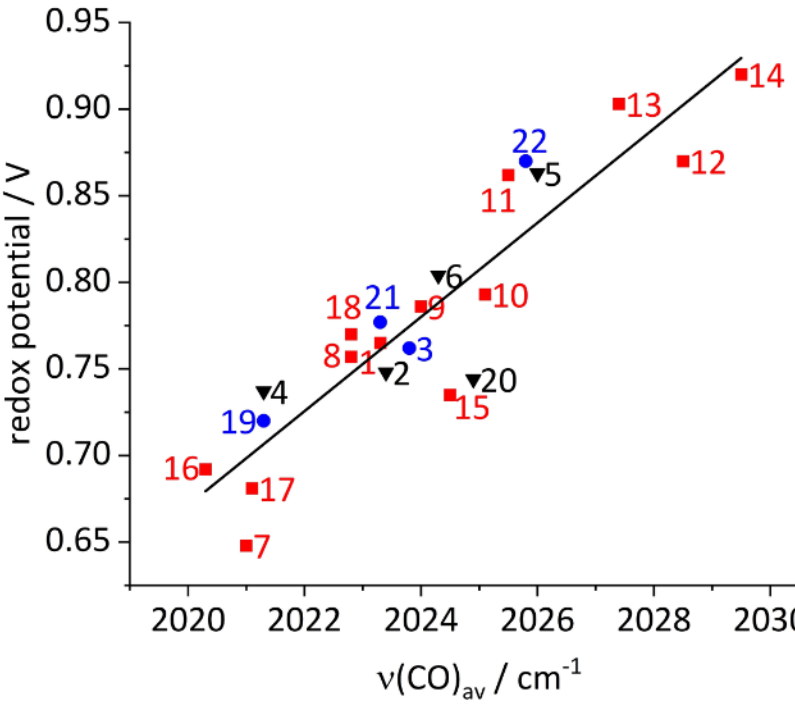

Figure 7. Plot of the redox potentials of [(NHC)IrCl(cod)] complexes vs. the average of ν(CO) for [(NHC)IrCl$(CO)_2$] in CH_2Cl_2. Color coding see legend to Figure 4.

using electron ionization (EI). UV-Vis spectra were recorded on Analytik Jena Specord 600 UV-Vis spectrometer, fluorescence spectra were recorded on *J*&M TIDAS S700/CCD UV/NIR 2098 spectrometer combined with *J*&M TIDAS LSM monochromator with 75 W Xenon light source and thermo-controlled cuvette holder. Samples for emission and absorption measurements were contained in 1 cm·1 cm quartz cuvette (Hellma Analytics). Cyclic voltammetry was performed using a standard electrochemical instrumentation consisted of an EG&G 273 A-2 potentiostat-galvanostat. A three-electrode configuration was employed. The working electrode was a Pt disk (diameter 1 mm) sealed in soft glass with a Pt wire as a counter electrode. The pseudo reference electrode was an Ag wire. Potentials were calibrated internally against the formal potential of ferrocene (+0.46 V vs. Ag/AgCl). All cyclic voltammograms were recorded in dry 1,2-dichloroethane under an atmosphere of argon, supporting electrolyte N*n*Bu$_4$PF$_6$ (c = 0.1 mol/L).

Materials. All chemicals were purchased as reagent grade from commercial suppliers and used without further purification, unless otherwise noted. Tetrahydrofuran was dried under sodium and distilled under argon atmosphere. Toluene from Sigma-Aldrich (Lab. Reagent grade, 99.3%) was dried and purified.[47] All solvents were stored over molecular sieves (4 Å) under N_2. Preparative chromatography was performed using Merck silica 60 (0.063–0.02 mesh).

General Procedure A [(NHC)IrCl(cod)] formation. A vial was charged with the corresponding azolium salt (1.0 equiv), [IrCl(cod)]$_2$ (0.5 equiv) and K_2CO_3 (3.0 equiv). The resulting mixture was suspended in acetone (3.0 mL) and stirred for 20 h at 60 °C. After this time the solvent was removed in vacuo and dichloromethane added (3.0 mL). The mixture was filtered through a pad of silica. The residue was purified by flash chromatography (CH_2Cl_2) to afford the desired complex as a yellow microcrystalline solid.

General Procedure B [(NHC)IrCl(cod)] formation. Azolium salt (1.8 equiv) and KO^{t}Bu (2.0 equiv) were placed in a Schlenk tube, dissolved in dry THF (5 mL) under an atmosphere of N_2 and stirred for 30 min at room temperature. To this mixture was added the [IrCl(cod)]$_2$ (1.0 equiv). The reaction mixture was stirred for 4 h at room temperature and the solvent was evaporated in vacuo. The mixture was dissolved in CH_2Cl_2 and filtered through a pad of silica. The residue was purified by flash chromatography (CH_2Cl_2) to afford the desired complex as yellow microcrystalline solid.

General Procedure C [(NHC)IrCl(cod)] formation. Azolium salt (1.0 equiv) and Ag_2O (0.5 equiv) were placed in Schlenk tube and dissolved in dry CH_2Cl_2. The mixture was stirred overnight, changing color from a black slurry to a clear solution. Addition of [IrCl(cod)]$_2$ (0.5 equiv) gave a bright yellow solution. After stirring the solution for 3 h at room temperature the volatiles were evaporated in vacuo. The residue was purified by flash column chromatography (CH_2Cl_2) to afford the desired complex as yellow microcrystalline solid.

General Procedure D [(NHC)IrCl(CO)$_2$] formation. To a Schlenk tube equipped with stirring bar and septa, the corresponding [(NHC)IrCl(cod)] complex and CH_2Cl_2 (2 mL) were added. A balloon with CO was connected via cannula and CO was bubbled through the stirred solution for 30 min at room temperature. The volatiles were evaporated under reduced pressure, pentane (5 mL) was added and the suspension sonicated for 5 min. The solid material was filtered off and washed with another batch of pentane.

General procedure for the titration fluorescence experiments. All experiments were carried out in quartz cuvettes with path lengths of 10.0 mm. A cuvette was charged with 2000 μL of $1.00 \cdot 10^{-6}$ M solution of the respective [(NHC)Ir(bdpSO$_3$)(cod)] complex in toluene or 1,2-dichloroethane/toluene (1:1 or 2:1) or 1,2-dichloroethane. The temperature (25 °C) was adjusted using a thermostat. Portions of purified solvent or a solution of salt in 1,2-dichloroethane were added to the cuvette (typical range 5 μL–100 μL). After each aliquot, the fluorescence intensity was monitored. The next aliquot was added when the fluorescence level was found to remain constant after 30 s. The titration was terminated when addition of a new aliquot did not lead to further increase in the fluorescence. The fluorescence data were finally corrected for dilution of the sample. In order to obtain the respective fluorescence intensity for the fully separated ion pair an 8 M solution of NBu$_4$Br in 1,2-dichloroethane was added (10 μL, $8.00 \cdot 10^{-5}$ mol).

Acknowledgements

This work was supported by the Deutsche Forschungsgemeinschaft (DFG) via grant Pl 178/18-2. We wish to thank Dr. Roman Vasiuta for performing important initial experiments. Open Access funding enabled and organized by Projekt DEAL.

Conflict of Interest

The authors declare no conflict of interest.

Keywords: Fluorescence · Ion Pairing · Iridium · NHC ligands

[1] a) T. Dröge, F. Glorius, *Angew. Chem. Int. Ed.* **2010**, *49*, 6940–6952; *Angew. Chem.* **2010**, *122*, 7094–7107; b) H. V. Huynh, *Chem. Rev.* **2018**, *118*, 9457–9492; c) D. J. Durand, N. Fey, *Chem. Rev.* **2019**, *119*, 6561–6594; d) D. Cremer, E. Kraka, *Dalton Trans.* **2017**, *46*, 8323–8338; e) A. Gomez-Suarez, D. J. Nelson, S. P. Nolan, *Chem. Commun.* **2017**, *53*, 2650–2660.
[2] R. Dorta, E. D. Stevens, N. M. Scott, C. Costabile, L. Cavallo, C. D. Hoff, S. P. Nolan, *J. Am. Chem. Soc.* **2005**, *127*, 2485–2495.
[3] A. R. Chianese, X. Li, M. C. Janzen, J. W. Faller, R. H. Crabtree, *Organometallics* **2003**, *22*, 1663–1667.
[4] R. A. Kelly, H. Clavier, S. Giudice, N. M. Scott, E. D. Stevens, J. Bordner, I. Samardjiev, C. D. Hoff, L. Cavallo, S. P. Nolan, *Organometallics* **2008**, *27*, 202–210.
[5] S. Wolf, H. Plenio, *J. Organomet. Chem.* **2009**, *694*, 1487–1492.
[6] G. Ciancaleoni, N. Scafuri, G. Bistoni, A. Macchioni, F. Tarantelli, D. Zuccaccia, L. Belpassi, *Inorg. Chem.* **2014**, *53*, 9907–9916.
[7] a) S. Leuthäußer, D. Schwarz, H. Plenio, *Chem. Eur. J.* **2007**, *13*, 7195–7203; b) S. Leuthäußer, V. Schmidts, C. M. Thiele, H. Plenio, *Chem. Eur. J.* **2008**, *14*, 5465–5481.
[8] H. V. Huynh, Y. Han, R. Jothibasu, J. A. Yang, *Organometallics* **2009**, *28*, 5395–5404.
[9] K. Verlinden, H. Buhl, W. Frank, C. Ganter, *Eur. J. Inorg. Chem.* **2015**, *2015*, 2416–2425.
[10] D. Marchione, M. A. Izquierdo, G. Bistoni, R. W. A. Havenith, A. Macchioni, D. Zuccaccia, F. Tarantelli, L. Belpassi, *Chem. Eur. J.* **2017**, *23*, 2722–2728.
[11] O. Back, M. Henry-Ellinger, C. D. Martin, D. Martin, G. Bertrand, *Angew. Chem. Int. Ed.* **2013**, *52*, 2939–2943; *Angew. Chem.* **2013**, *125*, 3011–3015.
[12] A. Liske, K. Verlinden, H. Buhl, K. Schaper, C. Ganter, *Organometallics* **2013**, *32*, 5269–5272.
[13] S. V. C. Vummaleti, D. J. Nelson, A. Poater, A. Gomez-Suarez, D. B. Cordes, A. M. Z. Slawin, S. P. Nolan, L. Cavallo, *Chem. Sci.* **2015**, *6*, 1895–1904.
[14] D. Gatineau, D. Lesage, H. Clavier, H. Dossmann, C. H. Chan, A. Milet, A. Memboeuf, R. B. Cole, Y. Gimbert, *Dalton Trans.* **2018**, *47*, 15497–15505.
[15] H. Clavier, S. P. Nolan, *Chem. Commun.* **2010**, *46*, 841–861.

[16] A. Poater, B. Cosenza, A. Correa, S. Giudice, F. Ragone, V. Scarano, L. Cavallo, *Eur. J. Inorg. Chem.* **2009**, 1759–1766.
[17] Different default radii and different metal-C(NHC) values have also been employed, which leads to some arbitrarity in the buried volume values.
[18] D. G. Gusev, *Organometallics* **2009**, *28*, 6458–6461.
[19] L. Falivene, R. Credendino, A. Poater, A. Petta, L. Serra, R. Oliva, V. Scarano, L. Cavallo, *Organometallics* **2016**, *35*, 2286–2293.
[20] L. Falivene, Z. Cao, A. Petta, L. Serra, A. Poater, R. Oliva, V. Scarano, L. Cavallo, *Nat. Chem.* **2019**, *11*, 872–879.
[21] A. V. Brethomé, S. P. Fletcher, R. S. Paton, *ACS Catal.* **2019**, *9*, 2313–2323.
[22] D. J. Durand, N. Fey, *Acc. Chem. Res.* **2021**, *54*, 837–848.
[23] a) P. Kos, H. Plenio, *Chem. Eur. J.* **2015**, *21*, 1088–1095; b) O. Halter, I. Fernández, H. Plenio, *Chem. Eur. J.* **2017**, *23*, 711–719; c) O. Halter, H. Plenio, *Eur. J. Inorg. Chem.* **2018**, 2935–2943; d) P. Kos, H. Plenio, *Angew. Chem. Int. Ed.* **2015**, *54*, 13293–13296; *Angew. Chem.* **2015**, *127*, 13491–13494; e) O. Halter, J. Spielmann, Y. Kanai, H. Plenio, *Organometallics* **2019**, *38*, 2138–2149.
[24] O. Halter, R. Vasiuta, I. Fernández, H. Plenio, *Chem. Eur. J.* **2016**, *22*, 18066–18072.
[25] L. Li, J. Han, B. Nguyen, K. Burgess, *J. Org. Chem.* **2008**, *73*, 1963–1970.
[26] a) R. Savka, H. Plenio, *Dalton Trans.* **2015**, *44*, 891–893; b) P. J. Rayner, P. Norcott, K. M. Appleby, W. Iali, R. O. John, S. J. Hart, A. C. Whitwood, S. B. Duckett, *Nat. Commun.* **2018**, *9*, 4251.
[27] G. Sipos, P. Gao, D. Foster, B. W. Skelton, A. N. Sobolev, R. Dorta, *Organometallics* **2017**, *36*, 801–817.
[28] A. Macchioni, *Chem. Rev.* **2005**, *105*, 2039–2074.
[29] This is based on the reasonable assumption, that the true close ion paired complexes would display the same fluorescence intensity.
[30] R. Savka, S. Foro, H. Plenio, *Dalton Trans.* **2016**, *45*, 11015–11024.
[31] a) M. Süßner, H. Plenio, *Chem. Commun.* **2005**, 5417–5419; b) V. Cesar, N. Lugan, G. Lavigne, *J. Am. Chem. Soc.* **2008**, *130*, 11286–11287; c) R. Credendino, L. Falivene, L. Cavallo, *J. Am. Chem. Soc.* **2012**, *134*, 8127–8135.
[32] a) C. Hansch, A. Leo, R. W. Taft, *Chem. Rev.* **1991**, *91*, 165–195; b) D. H. McDaniel, H. C. Brown, *J. Org. Chem.* **1958**, *23*, 420–427.
[33] T. Papp, L. Kollár, T. Kégl, *Chem. Phys. Lett.* **2013**, *588*, 51–56.
[34] Y. Zhang, V. Cesar, G. Storch, N. Lugan, G. Lavigne, *Angew. Chem. Int. Ed.* **2014**, *53*, 6482–6486; *Angew. Chem.* **2014**, *126*, 6600–6604.
[35] C. A. Urbina-Blanco, X. Bantreil, H. Clavier, A. M. Z. Slawin, S. P. Nolan, *Beilstein J. Org. Chem.* **2010**, *6*, 1120–1126.
[36] H. W. Gibson, J. W. Jones, L. N. Zakharov, A. L. Rheingold, C. Slebodnick, *Chem. Eur. J.* **2011**, *17*, 3192–3206.
[37] a) D. Zuccaccia, A. Del Zotto, W. Baratta, *Coord. Chem. Rev.* **2019**, *396*, 103–116; b) M. Trinchillo, P. Belanzoni, L. Belpassi, L. Biasiolo, V. Busico, A. D'Amora, L. D'Amore, A. Del Zotto, F. Tarantelli, A. Tuzi, D. Zuccaccia, *Organometallics* **2016**, *35*, 641–654.
[38] a) G. N. Lewis, M. Randall, *J. Am. Chem. Soc.* **1921**, *43*, 1112–1154; b) P. Debye, E. Hückel, *Z. Phys.* **1923**, *24*, 305–325.
[39] The relative fluorescence intensity is directly proportional to the "equilibrium constant".
[40] C. L. Perrin, *J. Chem. Educ.* **2017**, *94*, 669–672.
[41] Linear plots are historically important and better accessible to the eye. This is the reason, why a linear plot is also displayed, even though non-linear fits are convenient these days and often more precise - see ref. 40.
[42] The given value for corrected data corresponds to the deviation of fluorescence intensity from the linear fit, compensating for the electronic effect of the respective NHC.
[43] P. d. Frémont, N. M. Scott, E. D. Stevens, S. P. Nolan, *Organometallics* **2005**, *24*, 2411–2418.
[44] B. J. Truscott, D. J. Nelson, C. Lujan, A. M. Z. Slawin, S. P. Nolan, *Chem. Eur. J.* **2013**, *19*, 7904–7916.
[45] It should be mentioned, that in these DFT calculations a metal center was not included. The energies are only those of the plain carbene with different N-isopropyl group orientations.
[46] The value is based on the average of the symmetric and the antisymmetric CO stretch, both absorbances tend to be broad and the resolution limit of the spectrometer being 0.5 wavenumbers.
[47] K. M. Kadish, X. Mu, J. E. Anderson, *Pure Appl. Chem.* **1989**, *61*, 1823–1828.

Manuscript received: June 16, 2021
Revised manuscript received: July 16, 2021